A carbon conductive filament-induced robust resistive switching behavior for brain-inspired computing

Tianqi Yu[a], Dong Wang[a], Min Liu[a], Wei Lei[a], Suhaidi Shafie[b], Mohd Nazim Mohtar[b], Nattha Jindapetch[c], Paphavee van Dommelen[d], Zhiwei Zhao*[a]

[a] Joint International Research Laboratory of Information Display and Visualization, School of Electronic Science and Engineering, Southeast University, Nanjing 210096, People's Republic of China

*E-mail: Zhao_zw@seu.edu.cn

[b] Institute of Nanoscience and Nanotechnology, University Putra Malaysia, Serdang, Selangor, Malaysia

[c] Department of Electrical Engineering, Faculty of Engineering, Prince of Songkla University, Hat Yai, Songkhla, 90112, Thailand

[d] Division of Physical Science, Faculty of Science, Prince of Songkla University, Hat Yai Campus 15 Karnjanavanich, Hat Yai, Kohong District Songkhla, Thailand, 90110

To explore the microstructure of the prepared $MoTe_2$ film, TEMs are performed on the prepared samples. Obvious lattice fringes are observed in a TEM cross-sectional structure of the $MoTe_2$, as shown in Fig. S1a. Then, the FFTs are performed on a randomly selected area (yellow line area), as indicated in the inset. The FFTs reveal that there are three sets of diffraction spots in the $MoTe_2$, with the lattice spacings of 1.44, 2.31, and 2.54 Å, corresponding to the (203), (006) and (103) planes of the $MoTe_2$, respectively. The above measurement results are re-marked in the nanoscale randomly selected area of Fig. S1a. XPS narrow-scan spectra are performed to verify the elemental compositions and bonding types of Mo and Te, as shown in Fig. S1b. Two strong peaks located at 228.3 eV and 231.5 eV can be correlated with Mo $3d_{5/2}$ and Mo $3d_{3/2}$, respectively, which can be assigned to Mo-Te bonds. Similar peaks are located at 573.1 eV and 583.4 eV, corresponding to Te $3d_{5/2}$ and Te $3d_{3/2}$, which are also related to Mo-Te bonds. These results are consistent with previously reported results.[1, 2] For the XRD diffraction patterns, six peaks with different intensities can be observed as 30.1° (101), 35.4° (103), 38.9° (006), 49.4° (106), 60.5° (200) and 644° (203), respectively.[3, 4] as shown in Fig. S1c. Fig. S1d illustrates the

Raman spectrum for $MoTe_2$ thin film, measured at a laser wavelength of 523 nm, two typical strong peaks can be observed at 233.8 cm^{-1} and 291.1 cm^{-1}, corresponding to the E^1_{2g} mode (in-plane atoms oscillation) and B^1_{2g} mode (out-of-plane interaction). [1, 5]

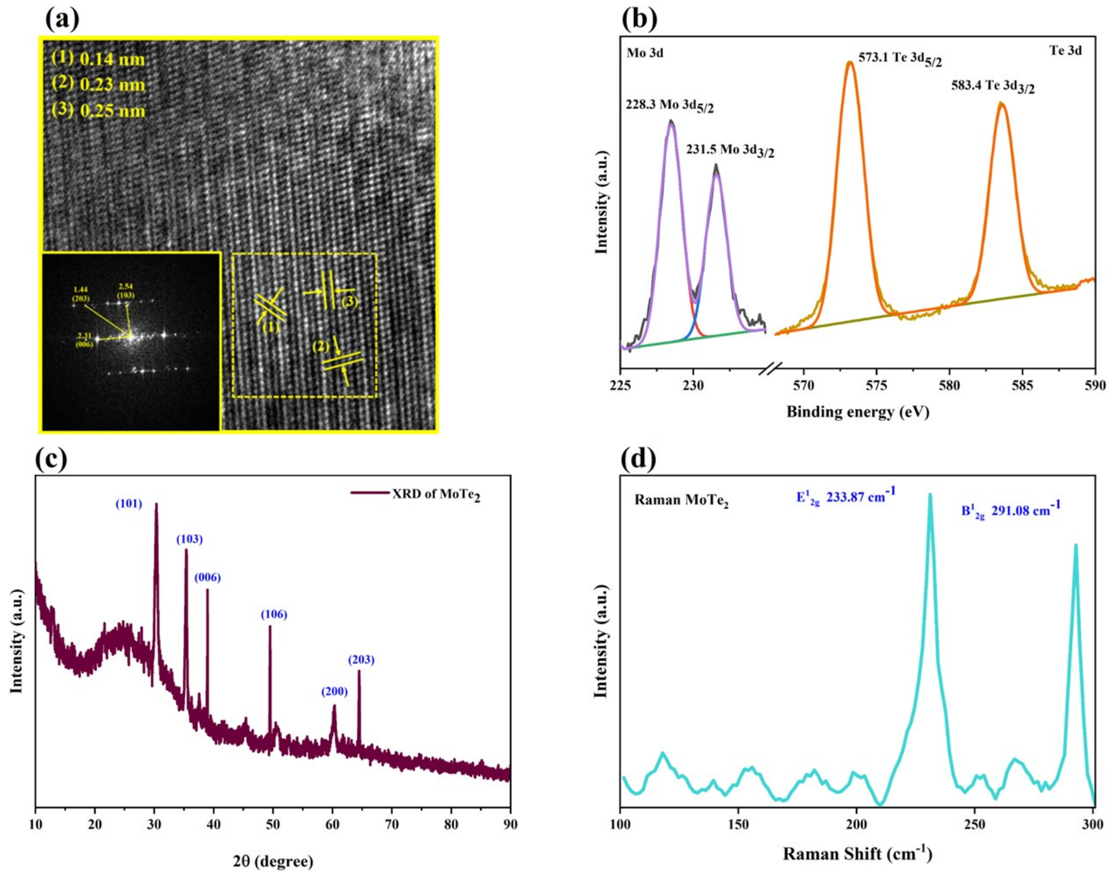

Fig. S1 Characterization of $MoTe_2$. (a) TEM image of $MoTe_2$ film, inset is the FFT image of the yellow area selected in Fig. S1a. (b) XPS spectrum of Mo 3d and Te 3d. (c) XRD 2θ-scans pattern of $MoTe_2$ film. (d) Raman spectrum of $MoTe_2$ film.

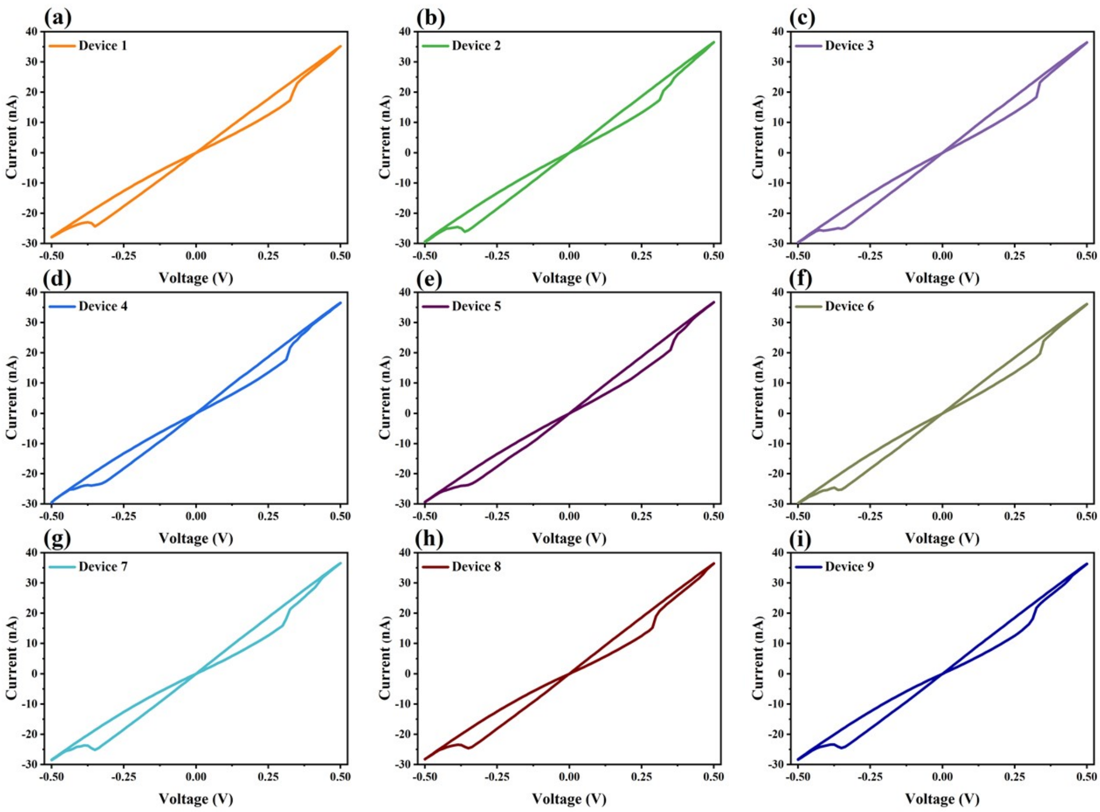

Fig. S2 I-V curves measured from nine devices in the same batch.

Fig. S3 shows the threshold voltage distribution of the nine randomly selected devices in Fig. S2. It can be found that it only fluctuates within a small range and does not affect the resistance state of the device.

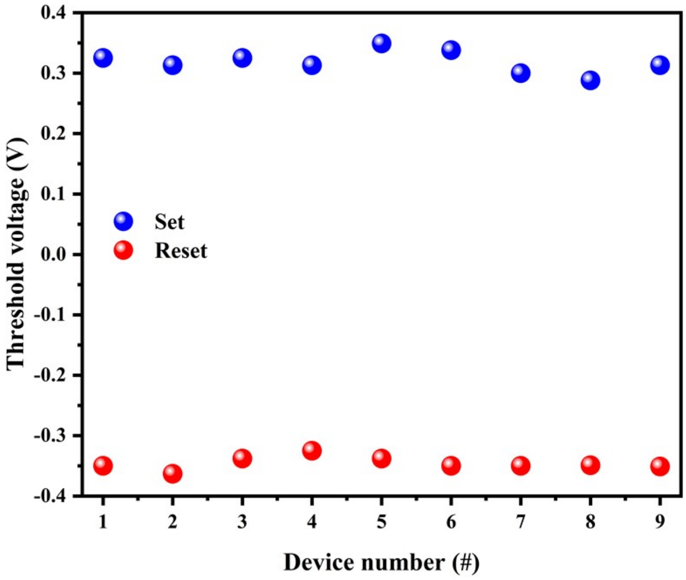

Fig. S3 Threshold voltage distribution of nine devices in the same batch.

Table S1 Compared with previously reported devices (Retention/ Endurance/ $V_{Set/Reset}$/ STDP/ PPF/ LTP/LTD)

No.	Device structure	Structure	Retention (s)	Endurance (N)	$V_{Set/Reset}$ (V)	STDP	PPF	LTP/LTD	Ref.
1	**$Pt/MoTe_2/CQDs/ITO$**	**Vertical**	**3×10^6**	**1×10^7**	**0.31/-0.34**	**Y**	**Y**	**Y**	**This work**
2	$Au/Ti/MoS_2/Ti/Au$	Planar	N	N	0.7/-0.5	N	N	N	6
3	Ag/h-BN/Cu	Vertical	3×10^3	550	-0.37/0.72	N	N	N	7
4	$Au/Ti/MoS_2/Ti/Au$	Planar	1.5×10^3	5×10^2	N	Y	Y	N	8
5	$W/MoS_2/p\text{-}Si$	Vertical	150	N	N	N	Y	Y	9
6	$Cu/MoS_2/Au$	Vertical	1×10^4	20	0.2/-0.3	Y	N	N	10
7	$Au/Ti/MoS_2/Ti/Au$	Planar	840	160	N	Y	N	Y	11
8	Au/h-BN/Au	Vertical	1×10^7	1×10^6	-1.5/3.2	N	N	N	12
9	$Au/Ag/MoS_2/Si$	Vertical	1×10^4	10	-0.3/0.4	Y	N	N	13
10	Pt/SnS/Pt	Planar	N	50	N	Y	Y	Y	14
11	$Au/NbO_x/NbS_2/MoS_2/Au$	Vertical	N	1500	-1.1/1.2	N	N	Y	15
12	Pt/h-BN/Ag	Vertical	N	1×10^8	-0.1/0.3	N	N	N	16
13	$Ag/BNO_x/graphene$	Vertical	1×10^3	1×10^4	0.7/-0.2	N	N	N	17

14	Au/Li_xMoS_2/Au	Planar	N	N	N	N	N	Y	18
15	Au/GaSe/Au	Planar	1×10^4	5×10^3	N	N	N	N	19
16	Au/Ti/MoS_2/Ti/Au	Planar	N	N	N	N	N	Y	20
17	Ag/$CrPS_4$/Au	Vertical	N	1×10^2	0.4/-1.7	N	N	N	21
18	graphene/$MoS_{2-x}O_x$/graphene	Vertical	1×10^5	1×10^7	1/-1.2	N	N	N	22
19	Ag/WO_{3-x}/WSe_2/graphene	Vertical	N	N	N	N	Y	Y	23
20	Au/Ti/h-BN/graphene	Vertical	N	50	5.2/-3	N	N	N	24
21	Ti/Au/$MoTe_2$/Ti/Ni	Vertical	1×10^3	N	1/-1.5	N	N	N	25
22	Pd/WSe_2/WO_3/Pd	Planar	N	N	N	N	Y	Y	26
23	Ag/MoO_2/Ag	Planar	1×10^4	8×10^2	0.6.-0.24	N	N	N	27
24	Ag/graphdiyne film/ITO	Vertical	1×10^3	N	1.3/-0.84	N	N	N	28
25	Ag/$2DP_{BTA+PDA}$/ITO	Vertical	3.5×10^4	200	1.5/-3.3	N	N	N	29
26	Ag/MP/ITO	Vertical	1×10^3	1×10^4	0.6/N	N	N	N	30
27	Ag/2D/3D perovskite/Pt/Ti	Vertical	N	2700	0.18/-0.11	N	N	N	31
28	Al/polymer membrane/ITO	Vertical	1×10^4	20	-1/3	N	N	N	32
29	Al/hollow MEH-PPV/2D CMP/ITO	Vertical	3×10^4	50	2.2/-2.9	N	N	N	33

30	Ag/MoS_2/polymer/Au	Vertical	1×10^3	300	0.4/-0.4	N	N	N	34

Table S2 Compared with previously reported devices (V_{set}/ V_{reset}/|C_v of V_{set}|/|C_v of V_{reset}|)

No.	**Device structure**	**Method**	**V_{set} (V)**	**V_{reset} (V)**	**|C_v of V_{set}|**	**|C_v of V_{reset}|**	**Ref.**
1	**Pt/$MoTe_2$/CQDs/ITO**	**Spin-coating**	**0.31**	**-0.34**	**3.9 %**	**1.18 %**	**This work**
2	Ti/$PdSeO_x$/$PdSe_2$/Au	Ozone treatment	0.7	-0.9	4.8 %	3.6 %	35
3	Al/WS_2/MoS_2/ITO	Solid-state sulfurization	0.7	-0.8	21 %	45 %	36
4	Ag/ZnO/WS_2/Al	Physical sputtering	1.4	-1.4	N	N	37
5	Ag/ZrO_2/WS_2/Pt	Spin-coating Physical sputtering	0.16	-0.06	3.8 %	13.3 %	38
6	Pt/HfO_2/TiO_x/TiN	Physical sputtering	0.75	-0.75	7.3 %	3.6 %	39
7	ITO/TiO_2/HfO_2/Pt	Physical sputtering	1.8	-1.5	2.8 %	2.7 %	40
8	Pt/HfO_2/Al_2O_3/W	ALD	1.43	-0.54	18.9 %	12.9 %	41
9	Graphene/$MoS_{2-x}O_x$/Graphene	Mechanical exfoliation air annealing	1.2	-1	N	N	22
10	Ti/h-BN/Au	CVD	1.8	-0.8	N	N	42
11	Au/h-BN/Au	CVD	2.7	-0.9	2 %	9.6 %	43
12	Ti/h-BN/Au	CVD	0.66	-0.41	22.7 %	12.2 %	44

13	Au/MoS_2/Au	CVD	1	-1.25	N	N	45
14	Cu/MoS_2/Au	CVD	0.25	-0.15	N	N	10
15	Ag/WS_2/Pt	Spin-coating	3.12	-2.93	N	N	38
16	Ti/a-BN/Si	Physical sputtering	3.1	-1.7	3.2 %	12.2 %	46
17	Ta/TaO_x/Pt	ALD	-0.55	0.94	10.9 %	5.3 %	47
18	Pt/0% dopedAl-HfO_2/TiN	ALD	-1	0.78	9.3 %	9.3 %	48
19	Pt/9.8% dopedAl-HfO_2/TiN	ALD	-1.58	0.69	18.8 %	9.8 %	48
20	Pt/16.5% dopedAl-HfO_2/TiN	ALD	-1.64	0.67	16.3 %	6.7 %	48
21	Pt/31.8% dopedAl-HfO_2/TiN	ALD	-1.34	0.85	16.3 %	26.0 %	48
22	Pt/46.2% dopedAl-HfO_2/TiN	ALD	-1.15	1.08	10.9 %	15.8 %	48
23	Ag/ ZrO_2/Pt	Physical sputtering	0.64	-0.43	34.4 %	48.8 %	38
24	Ti/HfO_2/ Pt	ALD	1.3	-1.12	27.7 %	42.8 %	49
25	Pt/HfO_2/Ti/W	ALD	0.88	-0.38	12.5 %	21.0 %	41
26	Pt/HfO_2/W	ALD	1.75	-0.60	34.3 %	25 %	41
27	TiN/HfO_2/Pt	Physical sputtering	-1.31	1.54	11.5 %	17.5 %	50
28	Pt/Ti/SiO_2/Ni/Cr	Self-assembly	1.6	-0.77	11.3 %	13.0 %	51
29	Ag/SiO_2/Si	CVD	1.11	-0.47	51.5 %	31.8 %	52

30	Ag nanocones/SiO_2/Ag	CVD	0.27	-0.22	28.0 %	32.2 %	52

Table S3 Compared with previously reported devices (V_{set}/ V_{reset}/Set Power/Reset Power)

No.	**Device structure**	**CF type**	**V_{set} (V)**	**V_{reset} (V)**	**Set Power (W)**	**Reset Power (W)**	**Ref.**
1	**Pt/$MoTe_2$/CQDs/ITO**	**C**	**0.31**	**-0.34**	**10^{-9}**	**10^{-9}**	**This work**
2	Ag/TiO_2:Ag/pt	Ag	0.2	-0.3	10^{-4}	10^{-3}	53
3	Ag/Ta_2O_5/Pt	Ag	0.3	-0.06	10^{-5}	10^{-1}	54
4	Ag/SiO_2/Pt	Ag	0.36	-0.42	10^{-5}	10^{-2}	55
5	Ag/SiO_2/Pt	Ag	4	-2	10^{-6}	10^{-2}	56
6	Ag/SiGe/Si	Ag	3.6	-2	10^{-7}	10^{-4}	57
7	Ag/amorphous TiO_2/Pt	Ag	2.3	-2.3	10^{-5}	10^{-4}	58
8	Ag/a-LSMO/Pt	Ag	0.5	-0.25	10^{-3}	10^{0}	59
9	Cu/AlN/TiN	Cu	1.5	-0.8	10^{-5}	10^{-4}	59
10	Ag/AgInSbTe/Ta	Ag	-0.8	0.4	10^{-5}	10^{-4}	60

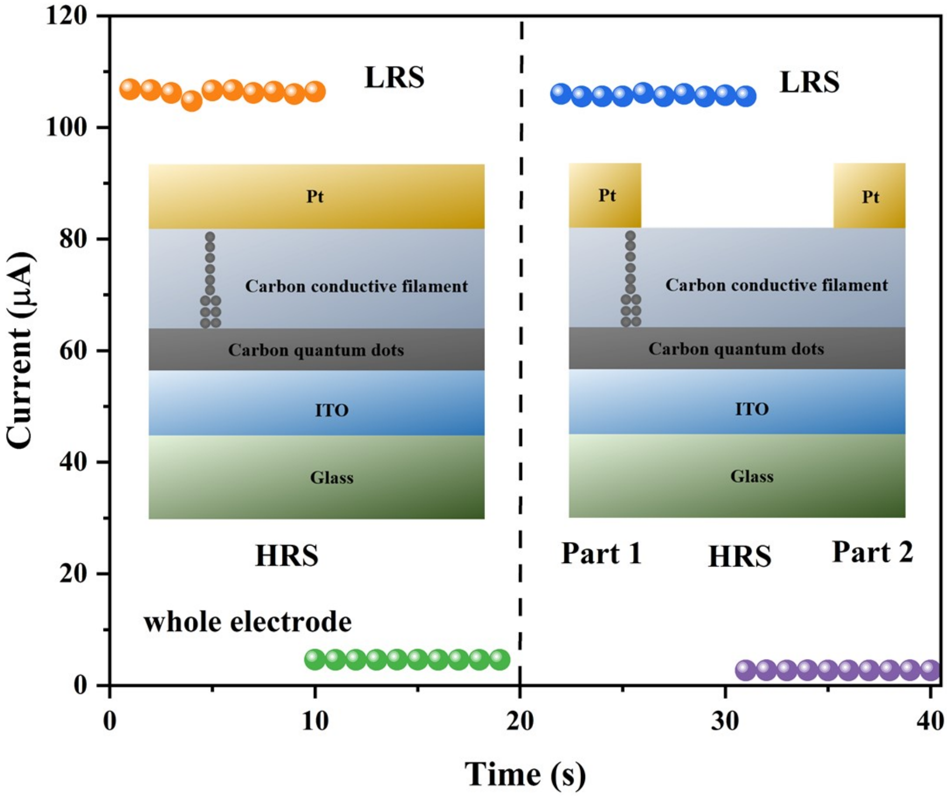

Fig. S4 Select different parts of the top electrode for electrical measurements.

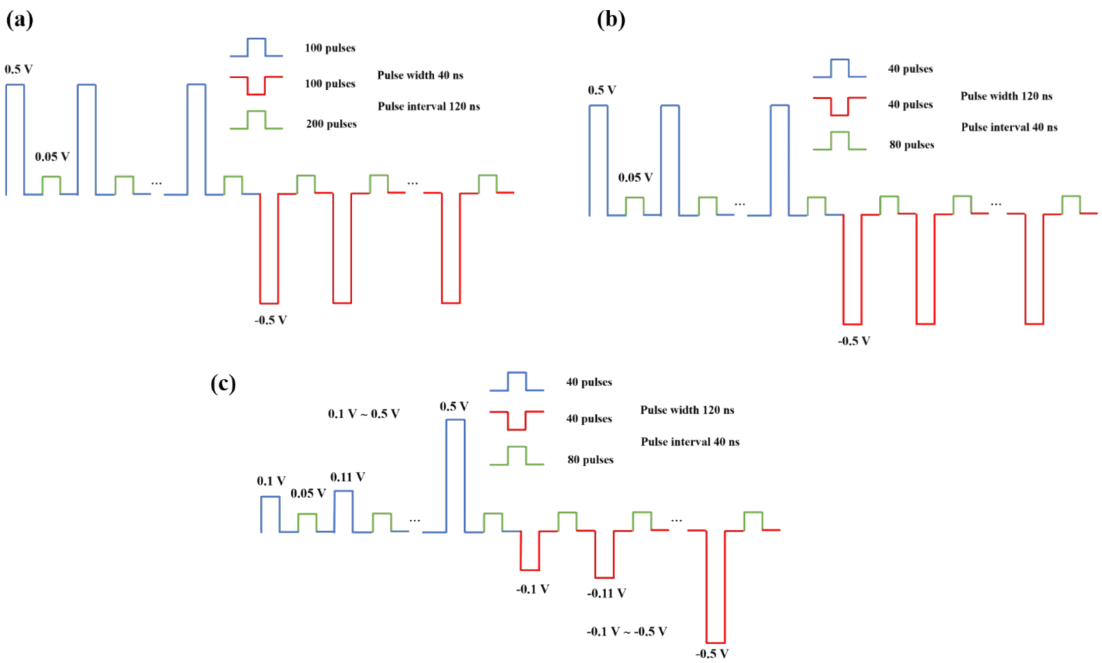

Fig. S5. The measurement waveforms utilized by the three pulse modes.

Table S4 Compared with previously reported devices (Accuracy)

No.	Device structure	Application	Accuracy	Ref.
1	**Pt/$MoTe_2$/CQDs/ITO**	**Handwritten digit recognition (MNIST)**	**96.9 %**	**This work**
2	Pd/Au/WO_x/SiO_2/W	Handwritten digit recognition (MNIST)	88.1 %	61
3	Au/Ti/GaO_x/Ti/Au	Fingerprint recognition (FVC 2002)	> 90 %	62
4	Au/$Cs_3Sb_2Br_9$/Au	Letters recognition	96 %	63
5	Ag/P_3HT@POM/Ag	Emotion pattern recognition	91.2 %	64
6	Ag/MoO_3/$CsPbI_2Br$/MoO_3/ITO	Handwritten digit recognition (MNIST)	88.7 %	65
7	Ag/$CsPbI_3$/Ag	Neural firing pattern recognition	87 %	66
8	Au/$NdNiO_3$/$LaAlO_3$/Pd	Handwritten digit recognition (MNIST)	> 80 %	67
9	Au/$MAPbI_3$/ITO	Fashion-MNIST Classification	90.1 %	68
10	Au/Cr/PEDOT:PF_6/Cr/Au	Flower pattern classification (Iris dataset)	96.7 %	69
11	Pd/SiOx:Ag/Ti/Pt	Handwritten digit recognition (MNIST)	83 %	70
12	Ag/OGB($CsPbBr_3$)/pTPD/PEDOT:PSS/ITO	Neural firing pattern recognition	85.1 %	71
13	Ag/PVP@Ag NW/Ag	Handwritten digit recognition (MNIST)	≈ 90.4 %	72
14	Ti/$PdSeO_x$/$PdSe_2$/Au	Handwritten digit recognition (MNIST)	93.4	35
15	Au/CQDs/ITO	Handwritten digit recognition (MNIST)	96.7 %	73

16	Ag/ZrO_2/WS_2/Pt	Handwritten digit recognition (MNIST)	87 %	38
17	Cr/Au/MoS_2/WO_3/SiO_2/Si	Handwritten digit recognition (MNIST)	93.2 %	74
18	Pt/BTO/NSTO	Handwritten digit recognition (MNIST)	96.4 %	75
19	Pt/BTO/LSMO/NSTO	Handwritten digit recognition (MNIST)	≈ 90 %	76
20	Ag/$Cs_3Cu_2I_5$/ITO	Handwritten digit recognition (MNIST)	94 %	77
21	Ag/IGZO/ITO	Handwritten digit recognition (MNIST)	91.2 %	78
22	Al/MXene-ZnO/ITO	Handwritten digit recognition (MNIST)	85 %	79
23	Al/MXene-ZnO/ITO	Image recognition	83 %	79
24	Ag/ P_3HT/perovskite/ ITO	Handwritten digit recognition (MNIST)	85.5 %	80
25	Ag/MoS_2/Pt	Handwritten digit recognition (MNIST)	90.37	81
26	Ag/$CH_3NH_3PbI_3$/ITO	Handwritten digit recognition (MNIST)	81.8 %	82
27	Au/SWCNTs/Au	Handwritten digit recognition (MNIST)	85.46 %	83
28	Pt/NbO/TiN	Handwritten digit recognition (MNIST)	95.7 %	84
29	Ni/SiN_x/AlO_y/TiN	Handwritten digit recognition (MNIST)	87.9 %	85
30	TiN/TaO_x/$HfAlO_y$/TiN	Arrhythmia detection	96.6 %	86

As an important learning rule in neural networks, STDP reflects the influence of the precise time (ΔT) between presynaptic spikes and postsynaptic spikes on synaptic weights (Fig. S5a). ΔT > 0 results in enhanced synaptic connectivity, known as long-term potentiation (LTP). In contrast, ΔT < 0 results in weakened connections between synapses, known as long-term depression (LTD).[87, 88] STDP can be fitted by the following formula:

$$\Delta W = Aexp\left(-\Delta T / \tau\right) + w_0 \tag{1}$$

where A is the scaling factor, τ is the time constant, and w_0 is the constant of the sub-association component. We demonstrate the STDP properties of the CQD-based memristor, as shown in Fig. S5b, and it can be found that the synaptic weight (ΔW) decreases with increasing ΔT. And the fitting parameters of STDP are counted, as shown in Table S5.

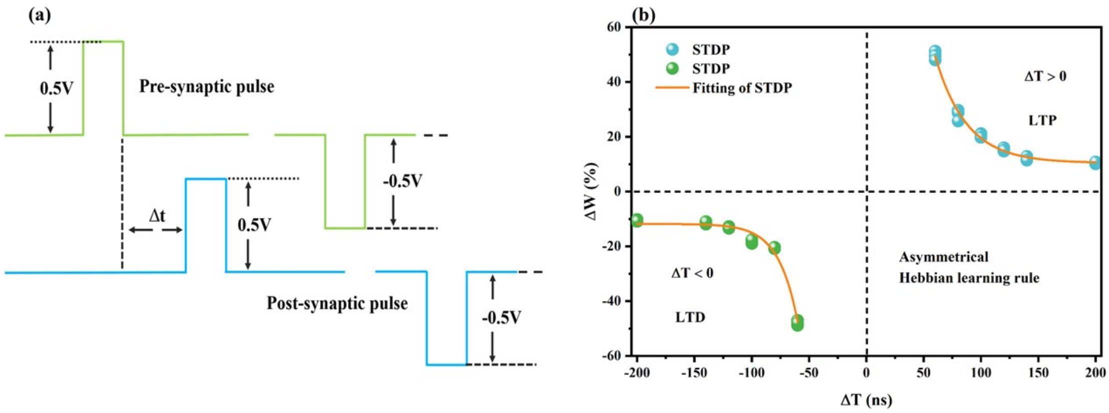

Fig. S6 STDP pulse waveform and characteristics of CQDs-based devices. (a) Programming pulse waveform selected for STDP measurement. (b) STDP characteristics of the CQDs-based memristors

Table S5 Spike-timing-dependent plasticity (STDP) fitting parameters of CQDs-based memristors

	STDP Asymmetric Hebbian learning rule	
	ΔT > 0	**ΔT < 0**
A	3.458	-13.221
τ	27.461	-16.628

Paired-pulse facilitation (PPF) refers to the summation of the biological synaptic input time. By changing the time interval (ΔT) between two consecutive input pulses, the simulation of information learning and forgetting behavior is realized.[89, 90] The PPF behavior can be reasonably fitted by the following formula:

$$PPF = C_1 \exp\left(-{}^{\Delta T}/_{\tau_1}\right) + C_2 exp({}^{\Delta T}/_{\tau_2}) \tag{2}$$

C_1 and C_2 are proportional constants, and τ_1 and τ_2 are time decay coefficients. The PPF properties of the CQD-based memristor are demonstrated in Figs. S6a and S6c. Obviously, the synaptic weight (ΔW) decreases with increasing ΔT. The programming pulse waveforms selected for PPF measurement are shown in Figs. S6b and S6d. And the fitting parameters of PPF are counted, as shown in Table S6.

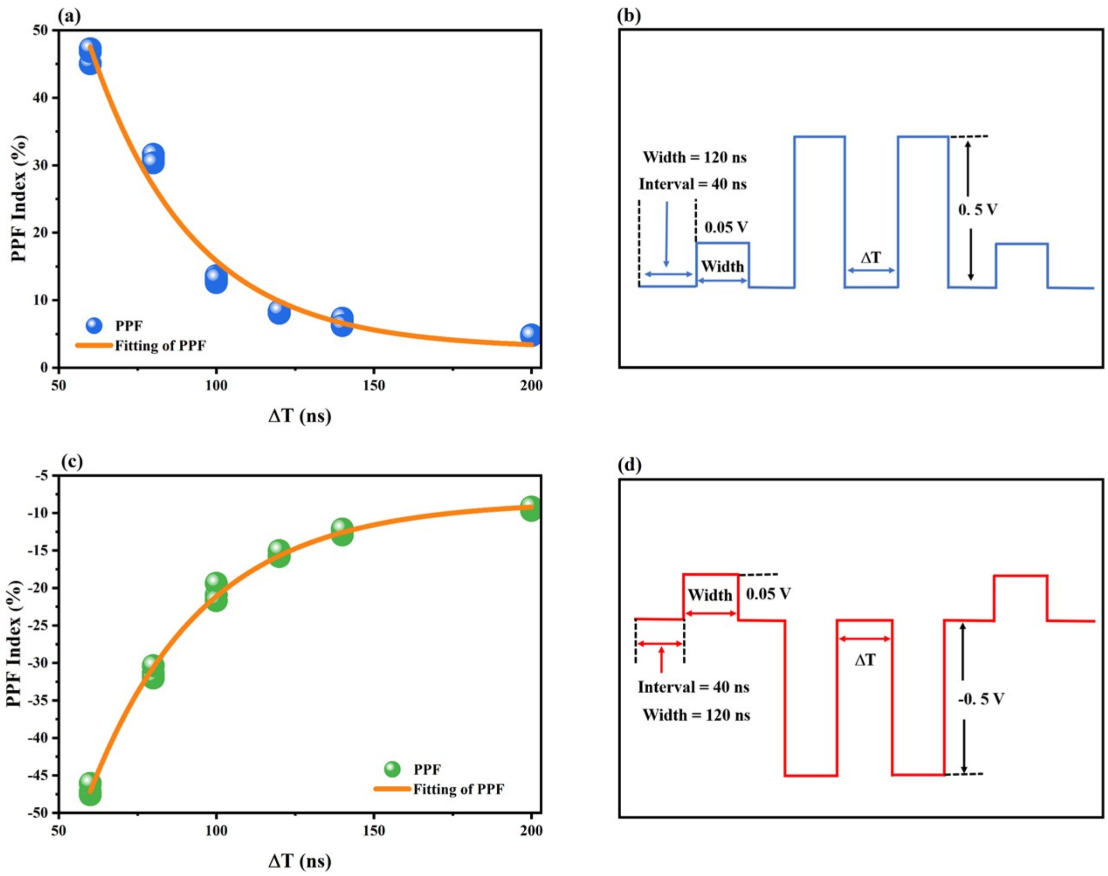

Fig. S7 PPF characteristics and pulse waveform of CQDs-based devices. (a, c) PPF characteristics of the CQDs-based memristors. (b, d) Programming pulse waveform selected for PPF measurement.

Table S6 Paired pulse facilitation (PPF) fitting parameters of CQDs-based memristors

	PPF	
	ΔT > 0	**ΔT < 0**
$\mathbf{C_1}$	8.739	-1.095
τ_1	32.417	35.894
$\mathbf{C_2}$	19.725	-0.965
τ_2	32.418	35.813

References

1. L. Zhou, K. Xu, A. Zubair, A. D. Liao, W. Fang, F. Ouyang, Y. H. Lee, K. Ueno, R. Saito, T. Palacios, J. Kong and M. S. Dresselhaus, *J Am Chem Soc*, 2015, **137**, 11892-11895.
2. L. Yang, H. Wu, W. Zhang, X. Lou, Z. Xie, X. Yu, Y. Liu and H. Chang, *Adv Electron Mater*, 2019, **5**, 1900552.
3. Y. W. Longhui Qiu, Vilas G. Pol and Aharon Gedanken, *Inorg Chem*, 2004, **43**, 6061-6066.
4. A. Fernández García, V. Torres-Costa, O. de Melo, F. Agulló-Rueda, G. R. Castro and M. Manso Silvan, *Appl Surf Sci*, 2021, **546**, 149076.
5. B. Sirota, N. Glavin, S. Krylyuk, A. V. Davydov and A. A. Voevodin, *Sci Rep*, 2018, **8**, 8668.
6. J. O. Island, S. I. Blanter, M. Buscema, H. S. J. van der Zant and A. Castellanos-Gomez, *Nano Lett*, 2015, **15**, 7853-7858.
7. K. Qian, R. Y. Tay, V. C. Nguyen, J. Wang, G. Cai, T. Chen, E. H. T. Teo and P. S. Lee, *Adv Funct Mater*, 2016, **26**, 2176-2184.
8. V. K. Sangwan, H. S. Lee, H. Bergeron, I. Balla, M. E. Beck, K. S. Chen and M. C. Hersam, *Nature*, 2018, **554**, 500-504.
9. H. K. He, R. Yang, W. Zhou, H. M. Huang, J. Xiong, L. Gan, T. Y. Zhai and X. Guo, *Small*, 2018, **14**, e1800079.
10. R. Xu, H. Jang, M. H. Lee, D. Amanov, Y. Cho, H. Kim, S. Park, H. J. Shin and D. Ham, *Nano Lett*, 2019, **19**, 2411-2417.
11. L. Wang, W. Liao, S. L. Wong, Z. G. Yu, S. Li, Y. F. Lim, X. Feng, W. C. Tan, X. Huang, L. Chen, L. Liu, J. Chen, X. Gong, C. Zhu, X. Liu, Y. W. Zhang, D. Chi and K. W. Ang, *Adv Funct Mater*, 2019, **29**, 1901106.
12. X. Wu, R. Ge, P. A. Chen, H. Chou, Z. Zhang, Y. Zhang, S. Banerjee, M. H. Chiang, J. C. Lee and D. Akinwande, *Adv Mater*, 2019, **31**, e1806790.
13. K. Ranganathan, M. Fiegenbaum-Raz and A. Ismach, *Adv Funct Mater*, 2020, **30**, 2005718.
14. K. C. Kwon, Y. Zhang, L. Wang, W. Yu, X. Wang, I. H. Park, H. S. Choi, T. Ma, Z. Zhu,

B. Tian, C. Su and K. P. Loh, *ACS Nano*, 2020, **14**, 7628-7638.
15. B. Wang, H. Luo, X. Wang, E. Wang, Y. Sun, Y. C. Tsai, H. Zhu, P. Liu, K. Jiang and K. Liu, *ACS Nano*, 2020, **14**, 175-184.
16. R. D. Nikam, K. G. Rajput and H. Hwang, *Small*, 2021, **17**, e2006760.
17. H. Zhao, Z. Dong, H. Tian, D. DiMarzi, M. G. Han, L. Zhang, X. Yan, F. Liu, L. Shen, S. J. Han, S. Cronin, W. Wu, J. Tice, J. Guo and H. Wang, *Adv Mater*, 2017, **29**, 11703232.
18. X. Zhu, D. Li, X. Liang and W. D. Lu, *Nat Mater*, 2019, **18**, 141-148.
19. Y. Yang, H. Du, Q. Xue, X. Wei, Z. Yang, C. Xu, D. Lin, W. Jie and J. Hao, *Nano Energy*, 2019, **57**, 566-573.
20. D. Li, B. Wu, X. Zhu, J. Wang, B. Ryu, W. D. Lu, W. Lu and X. Liang, *ACS Nano*, 2018, **12**, 9240-9252.
21. M. J. Lee, S. Lee, S. Lee, K. Balamurugan, C. Yoon, J. T. Jang, S.-H. Kim, D.-H. Kwon, M. Kim, J.-P. Ahn, D. H. Kim, J.-G. Park and B. H. Park, *NPG Asia Mater*, 2018, **10**, 23-30.
22. M. Wang, S. Cai, C. Pan, C. Wang, X. Lian, Y. Zhuo, K. Xu, T. Cao, X. Pan, B. Wang, S.-J. Liang, J. J. Yang, P. Wang and F. Miao, *Nature Electron*, 2018, **1**, 130-136.
23. H. Du, M. Tu, S. Luo, Y. Liu, X. Qiu, H. Lu, S. Li, S. Yuan, W. Huang, W. Jie and J. Hao, *Appl Phys Lett*, 2020, **116**, 253102.
24. H. Park, M. A. Mastro, M. J. Tadjer and J. Kim, *Adv Electron Mater*, 2019, **5**, 1900333.
25. F. Zhang, H. Zhang, S. Krylyuk, C. A. Milligan, Y. Zhu, D. Y. Zemlyanov, L. A. Bendersky, B. P. Burton, A. V. Davydov and J. Appenzeller, *Nat Mater*, 2019, **18**, 55-61.
26. H. K. He, R. Yang, H. M. Huang, F. F. Yang, Y. Z. Wu, J. Shaibo and X. Guo, *Nanoscale*, 2020, **12**, 380-387.
27. M. Tu, H. Lu, S. Luo, H. Peng, S. Li, Y. Ke, S. Yuan, W. Huang, W. Jie and J. Hao, *ACS Appl Mater Interfaces*, 2020, **12**, 24133-24140.
28. W. Li, J. Liu, Y. Yu, G. Feng, Y. Song, Q. Liang, L. Liu, S. Lei and W. Hu, *Mater Chem Front*, 2020, **4**, 1268-1273.
29. J. Liu, F. Yang, L. Cao, B. Li, K. Yuan, S. Lei and W. Hu, *Adv Mater*, 2019, **31**, e1902264.
30. Y. Song, J. Liu, W. Li, L. Liu, L. Yang, S. Lei and W. Hu, *Chem Commun (Camb)*, 2020, **56**, 6356-6359.
31. S. Lee, H. Kim, D. H. Kim, W. B. Kim, J. M. Lee, J. Choi, H. Shin, G. S. Han, H. W. Jang and H. S. Jung, *ACS Appl Mater Interfaces*, 2020, **12**, 17039-17045.
32. Z. Zhang, Y. Nie, W. Hua, J. Xu, C. Ban, F. Xiu and J. Liu, *RSC Adv*, 2020, **10**, 20900-20904.
33. Y. Yin, Z. Zhou, X. Wang, H. Mao, C. Ban, Y. Chen, J. Liu, Z. Liu and W. Huang, *ACS Appl Mater Interfaces*, 2020, **12**, 1103-1109.
34. J. Chai, S. Tong, C. Li, C. Manzano, B. Li, Y. Liu, M. Lin, L. Wong, J. Cheng, J. Wu, A. Lau, Q. Xie, S. J. Pennycook, H. Medina, M. Yang, S. Wang and D. Chi, *Adv Mater*, 2020, **32**, e2002704.
35. Y. Li, S. Chen, Z. Yu, S. Li, Y. Xiong, M. E. Pam, Y. W. Zhang and K. W. Ang, *Adv Mater*, 2022, **34**, e2201488.

36. W. Zhang, H. Gao, C. Deng, T. Lv, S. Hu, H. Wu, S. Xue, Y. Tao, L. Deng and W. Xiong, *Nanoscale*, 2021, **13**, 11497-11504.
37. M. Kumar, D. K. Ban, S. M. Kim, J. Kim and C. P. Wong, *Adv Electron Mater*, 2019, **5**, 1900467.
38. X. Yan, C. Qin, C. Lu, J. Zhao, R. Zhao, D. Ren, Z. Zhou, H. Wang, J. Wang, L. Zhang, X. Li, Y. Pei, G. Wang, Q. Zhao, K. Wang, Z. Xiao and H. Li, *ACS Appl Mater Interfaces*, 2019, **11**, 48029-48038.
39. W. Xiong, L. Q. Zhu, C. Ye, F. Yu, Z. Y. Ren and Z. Y. Ge, *Adv Electron Mater*, 2019, **5**, 1900439.
40. R. Zhang, H. Huang, Q. Xia, C. Ye, X. Wei, J. Wang, L. Zhang and L. Q. Zhu, *Adv Electron Mater*, 2019, **5**, 1800833.
41. E. Shahrabi, C. Giovinazzo, M. Hadad, T. LaGrange, M. Ramos, C. Ricciardi and Y. Leblebici, *Adv Electron Mater*, 2019, **5**, 1800835.
42. Y. Shi, X. Liang, B. Yuan, V. Chen, H. Li, F. Hui, Z. Yu, F. Yuan, E. Pop, H. S. P. Wong and M. Lanza, *Nature Electron*, 2018, **1**, 458-465.
43. S. Chen, M. R. Mahmoodi, Y. Shi, C. Mahata, B. Yuan, X. Liang, C. Wen, F. Hui, D. Akinwande, D. B. Strukov and M. Lanza, *Nature Electron*, 2020, **3**, 638-645.
44. H. Jeong, J. Kim, D. Y. Kim, J. Kim, S. Moon, O. F. Ngome Okello, S. Lee, H. Hwang, S. Y. Choi and J. K. Kim, *ACS Appl Mater Interfaces*, 2020, **12**, 46288-46295.
45. R. Ge, X. Wu, M. Kim, J. Shi, S. Sonde, L. Tao, Y. Zhang, J. C. Lee and D. Akinwande, *Nano Lett*, 2018, **18**, 434-441.
46. J. Lee, J. H. Ryu, B. Kim, F. Hussain, C. Mahata, E. Sim, M. Ismail, Y. Abbas, H. Abbas, D. K. Lee, M. H. Kim, Y. Kim, C. Choi, B. G. Park and S. Kim, *ACS Appl Mater Interfaces*, 2020, **12**, 33908-33916.
47. D. S. Kuzmichev, Y. Y. Lebedinskii, C. S. Hwang and A. M. Markeev, *Phys Status Solidi-R*, 2018, **12**, 1800429.
48. S. Roy, G. Niu, Q. Wang, Y. Wang, Y. Zhang, H. Wu, S. Zhai, P. Shi, S. Song, Z. Song, Z.-G. Ye, C. Wenger, T. Schroeder, Y.-H. Xie, X. Meng, W. Luo and W. Ren, *ACS Appl Mater Interfaces*, 2020, **12**, 10648-10656.
49. J. Wang, L. Li, H. Huyan, X. Pan and S. S. Nonnenmann, *Adv Funct Mater*, 2019, **29**, 1808430.
50. S. Petzold, A. Zintler, R. Eilhardt, E. Piros, N. Kaiser, S. U. Sharath, T. Vogel, M. Major, K. P. McKenna, L. Molina-Luna and L. Alff, *Adv Electron Mater*, 2019, **5**, 1900484.
51. B. K. You, W. I. Park, J. M. Kim, K.-I. Park, H. K. Seo, J. Y. Lee, Y. S. Jung and K. J. Lee, *ACS Nano*, 2014, **8**, 9492-9502.
52. B. K. You, J. M. Kim, D. J. Joe, K. Yang, Y. Shin, Y. S. Jung and K. J. Lee, *ACS Nano*, 2016, **10**, 9478-9488.
53. X. Yan, J. Zhao, S. Liu, Z. Zhou, Q. Liu, J. Chen and X. Y. Liu, *Adv Funct Mater*, 2018, **28,** 1705320.
54. T. Tsuruoka, T. Hasegawa, K. Terabe and M. Aono, *Nanotechnology*, 2012, **23**, 435705.
55. Y. Sun, C. Song, J. Yin, X. Chen, Q. Wan, F. Zeng and F. Pan, *ACS Appl Mater Interfaces*, 2017, **9**, 34064-34070.
56. H. Sun, Q. Liu, C. Li, S. Long, H. Lv, C. Bi, Z. Huo, L. Li and M. Liu, *Adv Funct Mater*,

2014, **24**, 5679-5686.
57. S. Choi, S. H. Tan, Z. Li, Y. Kim, C. Choi, P. Y. Chen, H. Yeon, S. Yu and J. Kim, *Nat Mater*, 2018, **17**, 335-340.
58. B. G. Chae, J. B. Seol, J. H. Song, K. Baek, S. H. Oh, H. Hwang and C. G. Park, *Adv Mater*, 2017, **29,** 1701752.
59. D. Liu, H. Cheng, X. Zhu, G. Wang and N. Wang, *ACS Appl Mater Interfaces*, 2013, **5**, 11258-11264.
60. Y. Li, L. Xu, Y.-P. Zhong, Y.-X. Zhou, S.-J. Zhong, Y.-Z. Hu, L. O. Chua and X.-S. Miao, *Adv Electron Mater*, 2015, **1**, 1500125.
61. C. Du, F. Cai, M. A. Zidan, W. Ma, S. H. Lee and W. D. Lu, *Nature Commun*, 2017, **8**, 2204.
62. Z. Zhang, X. Zhao, X. Zhang, X. Hou, X. Ma, S. Tang, Y. Zhang, G. Xu, Q. Liu and S. Long, *Nature Commun,* 2022, **13**, 6590.
63. J.-Y. Mao, Z. Zheng, Z.-Y. Xiong, P. Huang, G.-L. Ding, R. Wang, Z.-P. Wang, J.-Q. Yang, Y. Zhou, T. Zhai and S.-T. Han, *Nano Energy*, 2020, **71**, 104616.
64. G. Zhang, Z. Y. Xiong, Y. Gong, Z. Zhu, Z. Lv, Y. Wang, J. Q. Yang, X. Xing, Z. P. Wang, J. Qin, Y. Zhou and S. T. Han, *Adv Funct Mater*, 2022, **32**, 2204721.
65. L.-W. Chen, W.-C. Wang, S.-H. Ko, C.-Y. Chen, C.-T. Hsu, F.-C. Chiao, T.-W. Chen, K.-C. Wu and H.-W. Lin, *Adv Intelligent Systems*, 2020, **3**, 2000196.
66. X. Zhu, Q. Wang and W. D. Lu, *Nature Commun*, 2020, **11**, 2439.
67. T. J. P. Hai-Tian Zhang, A. N. M. Nafiul Islam, Dat S. J. Tran, Sukriti Manna, Qi Wang, Sandip Mondal, Haoming Yu, Suvo Banik, Shaobo Cheng, Hua Zhou, Sampath Gamage, Sayantan Mahapatra, Yimei Zhu, Yohannes Abate, Nan Jiang, Subramanian K. R. S. Sankaranarayanan, Abhronil Sengupta, Christof Teuscher, Shriram Ramanathan, *Science*, 2022, **375**, 533.
68. J. Yang, F. Zhang, H.-M. Xiao, Z.-P. Wang, P. Xie, Z. Feng, J. Wang, J. Mao, Y. Zhou and S.-T. Han, *ACS Nano*, 2022, **16**, 21324-21333.
69. C. G. Matteo Cucchi, Lautaro Petrauskas, Peter Steiner, Hsin Tseng, and B. P. Axel Fischer, Christian Matthus, Peter Birkholz, Hans Kleemann, Karl Leo, *Sci Adv*, 2021, **7**, eabh0693.
70. R. Midya, Z. Wang, S. Asapu, X. Zhang, M. Rao, W. Song, Y. Zhuo, N. Upadhyay, Q. Xia and J. J. Yang, *Adv Intelligent Systems*, 2019, **1**, 1900084.
71. R. A. John, Y. Demirağ, Y. Shynkarenko, Y. Berezovska, N. Ohannessian, M. Payvand, P. Zeng, M. I. Bodnarchuk, F. Krumeich, G. Kara, I. Shorubalko, M. V. Nair, G. A. Cooke, T. Lippert, G. Indiveri and M. V. Kovalenko, *Nature Commun*, 2022, **13**, 2074.
72. G. Milano, G. Pedretti, K. Montano, S. Ricci, S. Hashemkhani, L. Boarino, D. Ielmini and C. Ricciardi, *Nature Mater*, 2021, **21**, 195-202.
73. T. Yu, Y. Fang, X. Chen, M. Liu, D. Wang, S. Liu, W. Lei, H. Jiang, S. Shafie, M. N. Mohtar, L. Pan and Z. Zhao, *Mater Horiz*, 2023, **10**, 2181-2190.
74. S. Hao, X. Ji, F. Liu, S. Zhong, K. Y. Pang, K. G. Lim, T. C. Chong and R. Zhao, *ACS Appl Nano Mater*, 2021, **4**, 1766-1775.
75. J. Li, C. Ge, J. Du, C. Wang, G. Yang and K. Jin, *Adv Mater*, 2020, **32**, e1905764.
76. J. Zhao, T. Yu, Y. Shao, R. Guo, W. Lin, G. Liu, Z. Zhou, Y. Pei, J. Wang, K. Sun, X. Yan and J. Chen, *Sci China Mater*, 2022, **66**, 1559-1568.

77. F. Zeng, Y. Guo, W. Hu, Y. Tan, X. Zhang, J. Feng and X. Tang, *ACS Appl Mater Interfaces*, 2020, **12**, 23094-23101.
78. H. Mao, Y. He, C. Chen, L. Zhu, Y. Zhu, Y. Zhu, S. Ke, X. Wang, C. Wan and Q. Wan, *Adv Electron Mater*, 2021, **8**, 2100918.
79. Y. Wang, Y. Gong, L. Yang, Z. Xiong, Z. Lv, X. Xing, Y. Zhou, B. Zhang, C. Su, Q. Liao and S. T. Han, *Adv Funct Mater*, 2021, **31**, 2100144.
80. X. Yang, Z. Xiong, Y. Chen, Y. Ren, L. Zhou, H. Li, Y. Zhou, F. Pan and S.-T. Han, *Nano Energy*, 2020, **78**, 105246.
81. K. Wang, L. Li, R. Zhao, J. Zhao, Z. Zhou, J. Wang, H. Wang, B. Tang, C. Lu, J. Lou, J. Chen and X. Yan, *Adv Electron Mater*, 2020, **6**, 1901342.
82. S. Ham, S. Choi, H. Cho, S.-I. Na and G. Wang, *Adv Funct Mater*, 2019, **29**, 1806646.
83. M. Li, Z. Xiong, S. Shao, L. Shao, S.-T. Han, H. Wang and J. Zhao, *Carbon*, 2021, **176**, 592-601.
84. W. Wang, R. Wang, T. Shi, J. Wei, R. Cao, X. Zhao, Z. Wu, X. Zhang, J. Lu, H. Xu, Q. Li, Q. Liu and M. Liu, *IEEE Electron Dev L*, 2019, **40**, 1407-1410.
85. S. Kim, H. Kim, S. Hwang, M. H. Kim, Y. F. Chang and B. G. Park, *ACS Appl Mater Interfaces*, 2017, **9**, 40420-40427.
86. Y. Zhong, J. Tang, X. Li, X. Liang, Z. Liu, Y. Li, Y. Xi, P. Yao, Z. Hao, B. Gao, H. Qian and H. Wu, *Nature Electron*, 2022, **5**, 672-681.
87. M. T. Sharbati, Y. Du, J. Torres, N. D. Ardolino, M. Yun and F. Xiong, *Adv Mater*, 2018, e1802353.
88. F. Ma, Y. Zhu, Z. Xu, Y. Liu, X. Zheng, S. Ju, Q. Li, Z. Ni, H. Hu, Y. Chai, C. Wu, T. W. Kim and F. Li, *Adv Funct Mater*, 2020, **30**, 1908901.
89. L. Hu, S. Fu, Y. Chen, H. Cao, L. Liang, H. Zhang, J. Gao, J. Wang and F. Zhuge, *Adv Mater*, 2017, **29**, 1606927.
90. L. Yang, M. Singh, S. W. Shen, K. Y. Chih, S. W. Liu, C. I. Wu, C. W. Chu and H. W. Lin, *Adv Funct Mater*, 2020, **31**, 2008259.